Journal of Cluster Science (2022) 33:163–171
https://doi.org/10.1007/s10876-020-01957-7

ORIGINAL PAPER

# Nanoparticles of two ZnO Precursors as an Encapsulating Matrix of Mangiferin: Associated Studies to Cytotoxic Effects on Liver Cancer Cells Hep-G2 and Healthy Lung Cell Beas-2B

Francisco Fabián Razura-Carmona[1] · Mayra Herrera-Martínez[2] · Sonia G. Sáyago-Ayerdi[1] · Alejandro Pérez-Larios[3] · Efigenia Montalvo-González[1] · Marco Vinicio Ramírez-Mares[4] · Jorge Alberto Sánchez-Burgos[1]

Received: 18 September 2020 / Accepted: 30 November 2020 / Published online: 2 January 2021


## Abstract

In recent years, metal oxides have been studied as an encapsulating matrix nevertheless, few studies the effect that can exist between different precursors to form this type of nanomaterials; In this paper, we compare its ability as a mangiferin (MG) nanoencapsulated. Phytochemical that has been studied for its generous biological properties like anti-inflammatory, antiproliferative, and others; the nanoparticles (NP's) be synthesized with zinc nitrate and zinc acetate. The results showed modifications in the morphology of the ZnO associated with the precursor but, there is no significant difference between any treatment that is associated with antitopoisomerase activity however, $ZnO_A$-MG is statistically the best treatment by reducing in greater proportion the production of COX-II prostaglandins (97.38 ± 7.09%) with a significant difference ($p < 0.05$) compared toCOX-I (68.02 ± 2.14%) but, it is not considered a selective treatment moreover $ZnO_A$-MG proved to be the least hepatotoxic (IC50, 140.19 ± 13.10 µg/mL) while $ZnO_N$ is the most cytotoxic for HEP-G2 and BEAS-2B ($IC_{50}$, 51.27 ± 4.72 and 26.91 ± 3.21 µg/mL). All treatments change the morphology of erythrocytes to low concentrations (25 µg/mL). Therefore the MG load benefits the biological impact of ZnO.

**Keywords** ZnO precursors · Mangiferin · Anticiclooxigenase · Antitopoisomerase and toxicity

## Introduction

Zinc oxide (ZnO) has been widely studied due to its optical properties, however, it has been observed that it can also be a good encapsulating matrix for its practical structural and physical applications [1, 2], therefore, in recent years the use in its potential application in the pharmaceutical and food industries has increased due to its low cost in synthesis [3]. To date, the best process to obtain nanometric size ZnO in dispersions has been the sol–gel route [4, 5], one of the techniques of design and synthesis of materials from molecular precursors such as alkoxides or inorganic sales, the development of metastable phases of mixed organo-inorganic solids to obtain three-dimensional particles [6]. Some of the studied applications of these structures as active constituents for topical creams, ointments, and lotions because they have been shown to possess a broad spectrum against microorganisms [7]. Nonetheless, other studies show that they not only prove effective for

✉ Jorge Alberto Sánchez-Burgos
jorgealberto_sanchezburgos@yahoo.com.mx;
jsanchezb@ittepic.edu.mx

[1] Laboratorio Integral de Investigación en Alimentos, Tecnológico Nacional de México/I.T.Tepic, Avenida Tecnológico No 2595, Lagos del Country, CP 63175 Tepic, Nayarit, Mexico

[2] Instituto de Farmacobiología, Universidad de la Cañada, Carretera Teotitlán-San Antonio Nanahuatipán, Km 1.7, Paraje Titlacuatitla, CP 68540 Teotitlán de Flores Magón, Oaxaca, Mexico

[3] Laboratorio de Investigación en Materiales, Agua y Energía, División de Ciencias Agropecuarias e Ingenierías, Centro Universitario de Los Altos, Universidad de Guadalajara, Av. Rafael Casillas Aceves 1200, CP 47620 Tepatitlán de Morelos, Jalisco, Mexico

[4] Departamento de Ingenierías Química y Bioquímica, Tecnológico Nacional de México/I.T.Morelia, Ave. Tecnológico 1500, Col. Lomas de Santiaguito, 58120 Morelia, Michoacan, Mexico

bacteria, but also show possible cytotoxic effect associated with the products generated during the synthesis of nanoparticles (NP's) [8], but this has not been a limitation to continue investigating more about them because some of the benefits offered by the development of nanostructures are that their peculiar size becomes a great advantage for the encapsulation of compounds with biological activity [9].

The chemical structures mostly secondary metabolites that have beneficial activity for humans, known as bioactive compounds (BC) have been one of the important targets for phytopharmacy since they have associated a large number of them with the improvement of clinical conditions [10, 11] only, one of disadvantages they present is their stability when ingested [12], for example is mangiferin (MG), the glucoxanthone obtained from the fruit or bark of the mango tree that has shown certain metabolic properties as an anti-inflammatory as a selective inhibitor of cyclooxygenase II (COX-II), antitumor (topoisomerase I (TOP-I) inhibitor), antiarthritic (α interferon inhibitor), and others [13–16]; this is why studies on the development of NP's loaded with BC in different encapsulating matrices have become somewhat repetitive, however, it is important to consider functional matrices and assess whether the integrity of the biological activity of phytochemicals is not compromised by synthesis of nanomaterials.

There are currently several studies focused on the optical properties of ZnO by the sol–gel method, and the comparison between the different types of particles obtained from the modifications of the method or by the change of precursors [17, 18]. In addition to this, products are generated in the different reactions of the synthesis such as olation and oxolation which can intervene in the development of the biological quality of NP's [19]. For this reason, in this work, two precursors of zinc oxide (acetate and zinc nitrate) were evaluated in order to corroborate if there are significant differences between them and as an encapsulating matrix of mangiferin on its activity Antitopoisomerase, anti-inflammatory, hepatotoxic and Cytotoxic in vitro effects.

## Materials and Method

Zinc acetate, zinc nitrate, polyethylene glycol (PEG), mangiferin, camptothecin (CPT), ethanol, ammonium hydroxide ($NH_4OH$), adenine and dimethylsulfoxide (DMSO) (Sigma-Aldrich Chemical), Biological material: Genetically modified *Saccharomyces cerevisiae* strains were donated by Dr. John Nitiss, of St. Jude Children's Research Hospital, Memphis, Tennessee; JN394 is deficient in DNA repair and permeability of medications (Matα ura3-52, leu2, trp1, his7, ade1-2, ISE2, rad52::LEU2), increases the sensitivity of these cells to medications and JN362a has exacerbated the mechanisms of DNA repair (Matα, ura3–52, leu2, trp1, his7, ade1–2, ISE2) [20, 21]. For the cell viability assays, the BEAS-2B cell lines (ATCC CRL-9609) immortalized cell line isolated from normal human bronchial epithelium were used, it has been used to evaluate the in vitro toxicity of some nanomaterials because it is a type of epithelial cell not cancerous and HEPG2 (ATCC HB-8065) hepatocellular carcinoma cell, is an established line, used as a model for drug metabolism and cytotoxicity studies because these cells show many characteristics of normal liver cells [22, 23], Dulbecco's Modified Eagle's Medium (DMEM) (Gibco 12320-032), fetal bovine serum (FBS) (JRScientific Inc., 43640-500), streptomycin/penicillin (PAA, P11-002). For the quantification of prostaglandins, a cyclooxygenase (COX ovine/human) Inhibitor Screening Assay inhibitor (Item No. 560131, Cayman Chemicals) was used.

### Synthesis

NP's were synthesized by the sol–gel method [24], Two treatments were obtained using zinc nitrate ($ZnO_N$) and zinc acetate ($ZnO_A$) as a precursor to ZnO and for the remaining two loaded treatments 10 mg of MG ($ZnO_N$-MG and $ZnO_A$-MG) was used. 2 g of PEG, 10 g organic salt, and MG (only for loaded treatments) were homogenized within 140 mL of ethanol, the solution was adjusted to pH 7 with $NH_4OH$, then the solution was heated with reflux (70 °C/3 h). The gel formed was dried (70 °C/24 h), The product was ground until a fine powder was obtained with a mortar, then the obtained xerogel was annealed at 500 °C/5 h under controlled atmosphere with a heat ramp of 1 °C/min and we ended up grinding again in a mortar until obtaining fine dust.

### Morphological Characterization

Scanning electron microscopy (SEM) was used to evaluate the surface morphology of the NP's (ETH, Zurich-Quanta 200F; The Netherlands). Before the analysis, the powders were suspended in ethanol in constant stirring, a drop was added to the appointment adhered to microscope disk, it was allowed to evaporate in a chamber with silica gel to prevent them from getting wet and later, 20 s of the gold coating was used by sputtering to obtain the best resolution of the material in the micrographs.

### Antitopoisomerase Activity

This assay was evaluated according to the methodology of Nitiss and Wang [20]. The treatments and CPT were suspended in DMSO [1 mg/mL]. The mutant strains JN362a

and JN394 were incubated in YPD medium added with 0.07% adenine (30 °C/18 h); for each treatment consisted of a volume of 3 mL of medium with cells in suspension [2 × $10^6$/mL cells in Logarithmic phase] and 50 µL of the treatment, were incubated (30 °C/24 h) in an orbital incubator (MaxQ4450, Thermo Scientific). As control of the effect of DMSO a vehicle treatment (Vh) was added, as negative control untreated (100% growth), the positive control was CPT topoisomerase I inhibitor. After the incubation time, a 100 µL aliquot of each treatment and controls was transferred to be inoculated in Petri dishes with YPDA medium, incubated (30 °C/48 h). The anti-topoisomerase activity was calculated by comparing the number of colonies counted in each treatment plate and the negative control that was considered as 100% growth. All experiments were performed in duplicate by three repetitions, the means and standard deviations of the population were calculated for each of the data and factorial statistical design $3^2$ involving three factors (ZnO precursor, load and strain) and two levels (zinc nitrate-zinc acetate, with-no load, and JN394-JN32a), the response variable was the percentage of growth of each yeast.

## Cyclooxygenase Inhibition

The samples were prepared at a concentration of 1 mg/mL subsequently, 10 µL of the solution, 160 µL of reaction buffer, 10 µL of Heme cofactor, and 10 µL of the corresponding enzyme were homogenized. The substrate (20 µL arachidonic acid) was also added to the mixture and homogenized for 10 min at 37 °C with subsequent stirring, tin chloride [83.3 mg/mL] was added to stop the reaction continuously, the samples were placed in cells of 96 wells. Then everything underwent a second reaction to estimate the formation of prostaglandins (PG), at this stage the Ellman's reagent was used, with which entrapment of formed prostaglandins will be made and will function as a linker in the endocrine receptors present in the reaction mixture, incubated for 18 h at 37 °C with oscillatory stirring. The plate was washed with 200 µL of the Ellmans reagent three times and finally incubated for 1 h, a reading was done at 415 nm in a microplate reader (Biotek, Synergy HT, Winooski VT, USA), Gen5 software. The percentage of cyclooxygenase inhibition was calculated based on the quantification of PG, considering an untreated sample as 100% generation of prostanoids, for this, PG was first quantified with a calibration curve [250,125,62.5, 31.25, 15.63 and 0 pg/mL]; The controls used were enzyme with heat treatment (100 °C/3 min) as 100% inhibition, positive control arachidonic acid [1 mg/mL] (AA+). This methodology was carried out for each enzyme with all samples and controls in triplicate. For the statistical design, factorial model $2^3$ was used involving three independent variables (ZnO precursor, charge, and enzyme), two levels respectively (zinc nitrate/zinc acetate, with/without charge and COX-I/COXII) a total of 8 treatments, the dependent variable was the percentage of inhibition [25, 26].

## Cell Viability

Cell lines are cultured in DMEM medium, supplemented with BFS [10%], and penicillin/streptomycin [1%] at 37 °C in a humid atmosphere with 5% $CO_2$. For hepatotoxicity and cytotoxicity studies, they will be used in 96-well microplates to which 100 µL of cell suspension (HEPG2 and BEAS-2B respectively) [1x$10^4$ cells/mL] are added, as negative control affects the untreated cell suspension, DMSO [10%] positive control. The treatments were administered in 8 serial dilutions [2500–19 µg/mL] in duplicate and three repetitions with which the concentration was obtained to inhibit 50% of the cell population; the volume was completed at 200 µL with medium supplemented in each well. Subsequently, the microplate was subjected to incubation at 37 °C in a humid atmosphere with 5% $CO_2$ for 72 h. Once this time was over, the medium was removed from each well, washed with 1X PBS three times, allowed to dry for 12 h and 50 µL of the same buffer, 50 µL of MTT [0.05%] was added, incubated at 37 °C in a humid atmosphere with 5% $CO_2$ for 4 h. Finally, 100 µL of DMSO was added, homogenized and the reading was done at 595 nm in a microplate reader (Biorad, iMark ™, Strasbourg, Schiltigheim, France). The percentage of cell viability of each of the treatments was obtained through Eq. (1). The factorial design $2^2$ for each line was performed separately with two factors (ZnO precursor and charge), two levels (zinc nitrate/zinc acetate and with/without load), and the study variable was the $IC_{50}$ obtained with the linear regression of the feasibility percentage of the concentrations used with Statistica version 12 (Dell StatSoft, USA) [27, 28].

$$Viability(\%) = \frac{ANC - AT}{ANC} \times 100 \quad (1)$$

where *ANC* Absorbance of negative control and *AT* Absorbance of treatment.

## Hemolysis

The assay was carried out in 100 µL of the washed erythrocyte suspension (1.2 × $10^6$ cell/mL) donated by the Pharmacobiology Laboratory of the Universidad de la Cañada, Oaxaca, Mexico; to which 100 µL of treatment was added, incubated (37 °C/1 h), centrifuged (800 rpm/3 min) and 100 µL of the supernatant was collected, this volume was placed in a 96-well microplate finally, a

reading was taken at 415 nm in a spectrophotometer (Biorad, iMark ™ Microplate Absorbance Reader), and the hemolysis percentage was quantified with the Eq. (2). All treatments followed this methodology ($ZnO_A$, $ZnO_N$, $ZnO_A$-MG, and $ZnO_N$-MG) using four different concentrations in physiological solution [25–200 mg/mL] based on the $IC_{50}$ obtained by cell line assays. The positive control was triton (T, 0.2%) and negative control saline solution (SS, 0.9%). The statistical experiment used was a factorial design $2^2$, two factors (ZnO precursor and charge), two levels (zinc nitrate–zinc acetate and with-no load) and the response variable used was the percentage of hemolysis [29]. Data were expressed as mean ± standard deviation (SD, n = 3). Statistical differences compared between treated groups and the untreated group was analyzed by one-way analysis of variance (ANOVA) and followed by Turkey HSD with Statistica version 12 (Dell StatSoft, USA).

$$Hemolysis(\%) = \frac{AT - ANC}{APC - ANC} \times 100 \quad (2)$$

where $AT$ absorbance of treatment, $ANC$ absorbance of negative control and $APC$ absorbance of positive control.

## Results and Discutients

### Scanning Electronic Microscopy

The micrographs shown in Fig. 1, correspond to controls and treatments. Figure 1a shows $ZnO_N$ NP's, they have a rounded structure with no apparent edges, their size is heterogeneous measuring less than 300 nm. On the other hand, uncharged control particles of the zinc acetate precursor ($ZnO_A$) (Fig. 1b), they have a completely non-spherical morphology as they appear to have edges forming a hexagon, larger than with the previous precursor. The preferential growth in the [0001] direction of the ZnO has been attributed to its polar axis [0001] [30]; given under conditions of moderate concentration of hydroxyl anions in the reaction medium. The irregular forms are attributed to preferential growth in the direction [0001] at a moderate pH of 7. Due to this, if there is an increase in pH, the concentration of zinc oxide ($Zn(OH)_4$) precursor increases, around the first ZnO nuclei, this change in the hydrogen potential in the suspension is attributed to the polarity of salts precursors and at the start of the reaction pH [31]. This leads to a development in several directions for the central axis of the core and the formation of flower-shaped particles is attributed to these conditions. On the contrary, the variation of polyethylene glycol restricts the growth in the radial direction for the nucleus, favoring the formation of spheres or rounded shape (seeds) [32]. $ZnO_N$-MG NP's (Fig. 1c) have greater homogeneity in size compared to $ZnO_N$. On the other hand, $ZnO_A$-MG (Fig. 1d), has a smaller size with respect to $ZnO_A$. This incidence on particle size compared to controls may be due to interactions formed in the nucleus with mangiferin during the synthesis. Recent studies reported encapsulating of a *Mangifera indica* L. extract in ZnO with zinc nitrate and, showed seed morphologies (like those shown in this study) with a size between 20 and 80 nm [33, 34].

### Antitopoisomerase Activity

During the exacerbated replication of cells, such as the development of carcinoma is also associated with a high cup of enzymes associated with this manifestation such as topoisomerases (TOPs), entrusted in the opening of DNA to carry out this phenomenon [35]. Some studies show that MG has inhibitory properties of these enzymes [13]. Therefore, it was considered to evaluate the antitopoisomerase activity to compare whether the effect of this BC maintains this effect even when encapsulated.

JN394 has a deficiency in DNA repair, so those substances that have a specific effect on the inhibition of TOPs the yeast will not grow, otherwise in JN362, having its DNA repair mechanisms exacerbated if the compound is specific in that type of damage (Antitopoisomerase) will grow normally. Figure 1 shows the percentage growth of the JN394 strains, finding that there are no significant differences between treatments $ZnO_A$ (− 35.45 ± 3.99%), $ZnO_N$ (38.93 ± 4.22%), $ZnO_A$-MG (33.22 ± 3.22%), $ZnO_N$-MG (35.23 ± 4.01%) as for JN362a $ZnO_A$ (− 28.93 ± 3.21%) $ZnO_N$ (30.05 ± 3.76%), $ZnO_A$-MG (26.21 ± 2.80%), $ZnO_N$-MG (28.33 ± 3.04%), there is also no effect between both strains; but, CPT (topoisomerase I inhibitor) exhibits differences related to treatments and between the two yeasts (JN394 −69.34 ± 7.22% and JN363a − 2.72 ± 0.40%) [36, 37], on the other hand, Vh did not have any type of activity i n this trial.

The topoisomerase effect of MG is possibly masked by the microbial effect of the oxide as shown in Fig. 2, since $ZnO_A$ and $ZnO_N$ are not charged and have the same behavior as those containing MG, it may be due to the concentration of BC in the treatment since, for each mg of the synthesized powder, there is approximately 142.85 ng. moreover, On the other hand, other studies detected an antimicrobial effect with a greater effect on bacteria, which have shown the nanometric size of the ZnO is not recognized by the bacteria and the entry of their system causes damage to the cell membrane, the DNA lost its ability to replication and cell proteins are deactivated [38, 39]; this is associated with the result in this experiment since both for the strain with DNA repair mechanisms and the one that

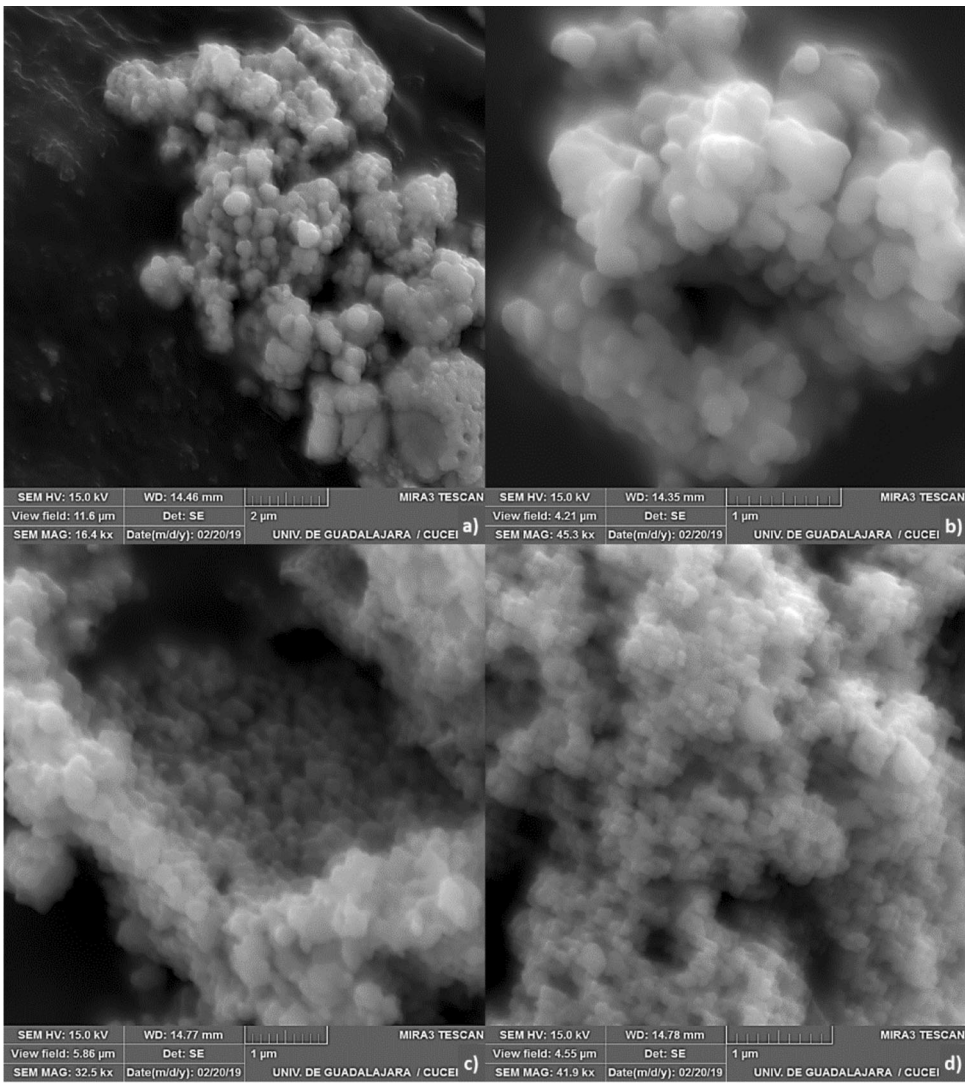


**Fig. 1** Scan electron micrographs of NP's controls **a** $ZnO_A$: Zinc acetate precursor NP's, **b** $ZnO_N$: Zinc nitrate precursor NP's, and charged nanoparticles **c** $ZnO_A$-MG: Zinc acetate precursor with mangiferin NP's, **d** $ZnO_N$-MG: Zinc nitrate precursor loaded mangiferin NP's

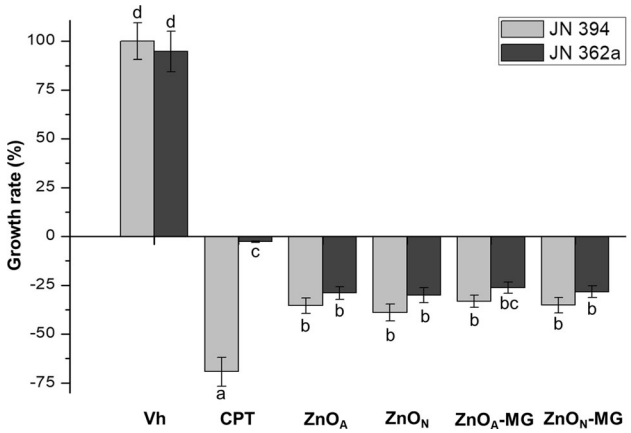


**Fig. 2** Growth percentage of strains JN394 and JN362a treated with NP's $ZnO_A$ (zinc acetate precursor), $ZnO_N$ (zinc nitrate precursor), $ZnO_A$-MG (zinc acetate and loaded with MG), $ZnO_N$-MG (zinc nitrate and loaded with MG) and controls Vh (DMSO 1.67%), CPT (camptotesin 50 µg)

was not resistantly decreased indistinctly. It has been discovered that this antibacterial potential varied among the gram-negative pathogenic microbes this might be due to variation in the structural architecture of bacterial cell wall and particle size surface area to volume ratio of ZnO even, the type of oxide precursor can show differences in the antibacterial activity [40].

## Cyclooxygenase Inhibition

Exist a significant difference between the inactive enzyme and the 100% active one; AA+ inhibited 99.83% compared to COX-I and 99.95% COX-II there is no significant difference from this non-selective COX-II anti-inflammatory [41]. The $ZnO_A$ and $ZnO_N$ treatments have no statistical difference between precursors, however, $ZnO_A$-MG and $ZnO_N$-MG have an effect between the loaded and unloaded, so MG has more contactless COX-II activity, The selective effect on the samples is modified with the type of

precursor as observed in $ZnO_A$-MG and $ZnO_N$-MG, shown increased production of COX-I prostanoids compared to COX-II in $ZnO_A$ however, $ZnO_A$-MG has a better activity as a treatment associated with inflammatory diseases, these results are displayed in Table 1.

It is important to indicate that although the powders received in its abundant composition ZnO, other components products of the synthesis of the material such as zinc nitrate and zinc acetate during the process of olation, Zn $(NO_3)_2 + NH_4OH = ZnOH + NH_4NO_3 + NO_3$ and Zn $(O_2C_2H_3)_2 + NH_4OH = ZnOH + NH_4CH_3CO_2$, which may be associated with statistics results by different salts since both acetate and ammonium nitrate have been considered to be enzyme inhibitors associated to albino rat metabolisms due to, are toxics [42]. Nevertheless, mangiferin has proven to be a selective COX-II inhibitor [43].

## Cell Viability

One of the most significant effects found on encapsulated treatments and those that were not loaded were observed in this trial because a significant difference was found in this factor (load), however, also the type of precursor affects cell viability, $ZnO_A$-MG ($IC_{50}$ 140.19 µg/mL) being the treatment that least hepatoxicity as seen in Fig. 3, the oxide obtained with zinc nitrate ($ZnO_N$) was significantly the most hepatotoxic ($IC_{50}$ 51.27 µg/mL), while those synthesized with zinc acetate ($ZnO_A$) showed greater viability ($IC_{50}$ 83.01 µg/mL), treatment with MG developed with salt that showed greater toxic effect for HEP-G2 ($ZnO_N$-MG) showed lower lethality than the unloaded ($ZnO_N$) ($IC_{50}$ 107.78 µg/mL). DMSO 10% showed to be harmful to this line (7.24 ± 0.97% viability), however, Vh did not interfere with the results (97.06 ± 1.52%).

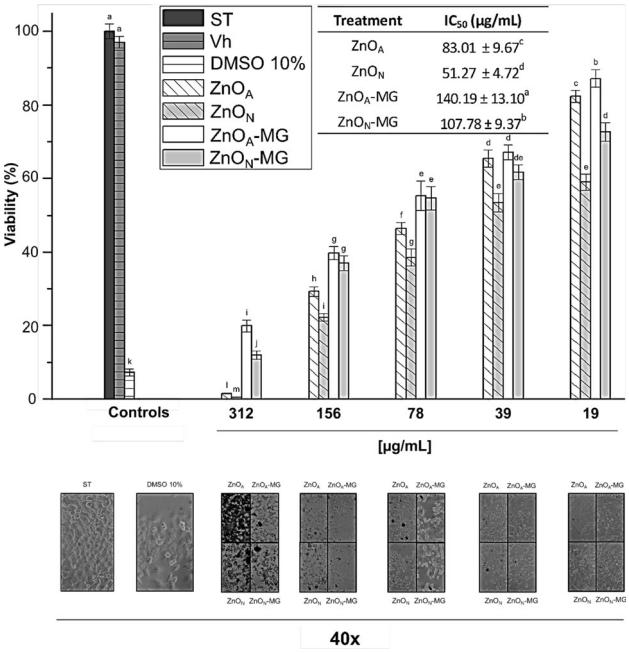


**Fig. 3** Viability percentage and $IC_{50}$ of the HEPG2 line treated with NP's $ZnO_A$ (zinc acetate precursor), $ZnO_N$ (zinc nitrate precursor), $ZnO_A$-MG (zinc acetate and loaded with MG), $ZnO_N$-MG (zinc nitrate and loaded with MG) and controls positive (DMSO 10%), Vh (DMSO 1%) and ST (only cell suspension)

**Table 1** Percentage of inhibition and concentration of cyclooxygenase prostaglandins I and II of each treatment and controls compared with acetylsalicylic acid (AA+)

| Enzyme | Treatment | Prostaglandin (pg/mL) | Inhibition (%) |
|---|---|---|---|
| COX-I | AA+ | 0.0269 ± 0.0019 | 99.83 ± 3.85[a] |
| | Inactive | 0.0628 ± 0.0039 | 99.61 ± 4.30[a] |
| | 100% active | 16.0613 ± 1.3380 | 0.11 ± 0.01[d] |
| | $ZnO_N$ | 0.0016 ± 0.0001 | 99.99 ± 1.00[a] |
| | $ZnO_A$ | 2.5361 ± 0.1963 | 84.21 ± 4.41[b] |
| | $ZnO_N$-MG | 1.5096 ± 0.1320 | 90.60 ± 6.01[b] |
| | $ZnO_A$-MG | 6.7423 ± 0.3460 | 58.02 ± 2.14[c] |
| COX-II | AA+ | 0.0844 ± 0.0067 | 99.95 ± 7.11[a] |
| | Inactive | 0.0751 ± 0.0049 | 99.96 ± 5.02[a] |
| | 100% active | 173.88 ± 9.01 | 0.83 ± 0.07[d] |
| | $ZnO_N$ | 0.0301 ± 0.0021 | 99.98 ± 6.99[a] |
| | $ZnO_A$ | 0.1060 ± 0.0087 | 99.94 ± 7.01[a] |
| | $ZnO_N$-MG | 2.5584 ± 0.2001 | 98.53 ± 9.00[a] |
| | $ZnO_A$-MG | 4.5632 ± 0.3029 | 97.38 ± 7.09[a] |

Results are expressed ± the standard deviation, 1 mg/mL acetylsalicylic acid (AA+), thermal stress enzyme (inactive), stress-free enzyme (100% active). Different superscript letters[a,b,c] indicate significative differences between groups per column. $ZnO_A$ (zinc acetate precursor), $ZnO_N$ (zinc nitrate precursor), $ZnO_A$-MG (zinc acetate and loaded with MG), $ZnO_N$-MG (zinc nitrate and loaded with MG)

Recent studies affected the hepatotoxic effect of ZnO at greater than 36 µg/mL and less than 16 µg/mL without damage by HEPG2 [44], effect of treatments is associated with ROS generated by ZnO in the medium at which caused an invasive effect of the dust at concessions greater than 312 µg/mL which caused cell death [45] According to the results, the only treatment that does not show a toxic effect for the cell line is $ZnO_A$-MG that exceeds the non-toxic limit for 200 nm materials [46], which shows that the MG load present in the oxide against arrest The effect of ROS being an antioxidant however, it is possible that the activity can be done because neutralized these reactive species.

The treatments in the same way as with HEPG2 showed a significant effect ($p < 0.05$) in both factors (precursor and load), however, the reported $IC_{50}$ is in a smaller portion to BEAS-2B, again $ZnO_A$-MG is the treatment with less cytotoxicity ($IC_{50}$ 72.13 µg/mL) followed by $ZnO_N$-MG and $ZnO_A$ ($IC_{50}$ 57.01 and 49.78 µg/mL) and ZnO-N

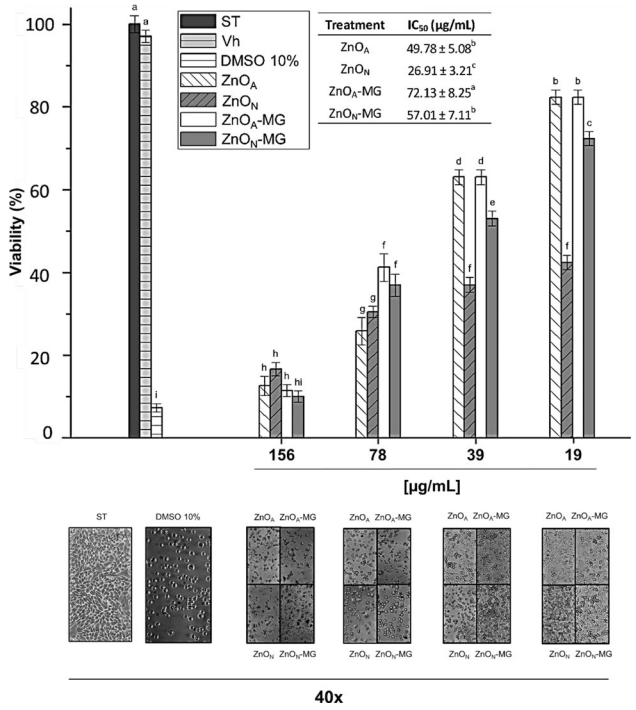


**Fig. 4** Viability percentage of the BEAS-2B line treated with NP's ZnO$_A$ (zinc acetate precursor), ZnO$_N$ (zinc nitrate precursor), ZnO$_A$-MG (zinc acetate and loaded with MG), ZnO$_N$-MG (zinc nitrate and loaded with MG) and controls positive (DMSO 10%), Vh (DMSO 1%) and ST (only cell suspension)

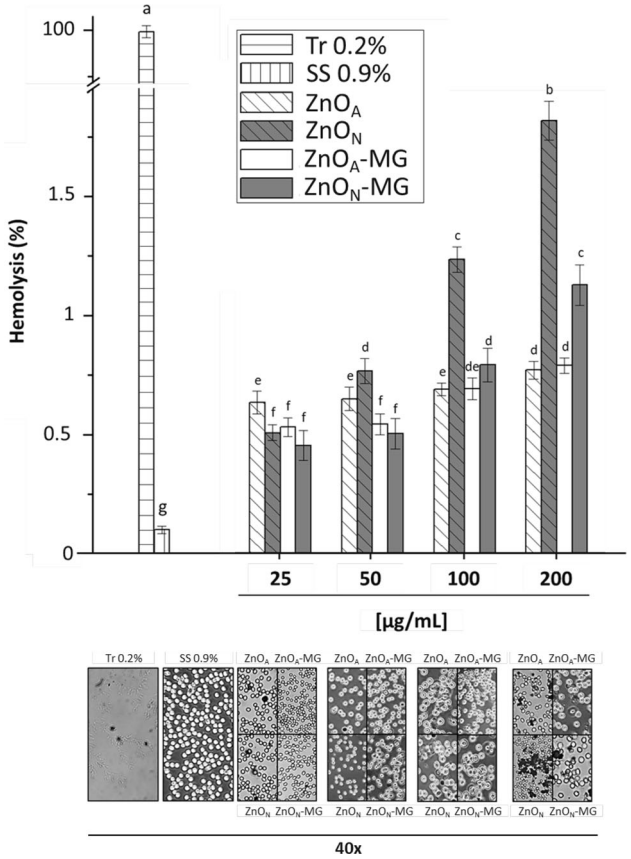


**Fig. 5** Percentage of hemolysis of NP's ZnO$_A$ (zinc acetate precursor), ZnO$_N$ (zinc nitrate precursor), ZnO$_A$-MG (zinc acetate and loaded with MG), ZnO$_N$-MG (zinc nitrate and loaded with MG) and controls Tr 0.2% (Triton), SS 09% (Saline solution)

is the sample that generated the most damage in the viability of this line (IC$_{50}$ 26.91 µg/mL).

Unlike liver cells, all treatments are toxic to BEAS-2B, ROS formed by ZnO prove cell death as shown in Fig. 4 however, the differences between precursors originate from the different products generated during the synthesis of the material [46, 47], since both acetate and ammonium nitrate have lethal effects for that line [48].

## Hemolysis

Based on the assay, the ability of a sample to generate damage to the membrane of a healthy enterocyte, the 4 treatments were added at lower and higher concentrations (25, 50, 100, and 200 µg/mL) than the IC$_{50}$ found in the viability tests independently, to evaluate their behavior in this tissue. The results are in Fig. 4, greater hemolysis effect is shown in the no-load treatment and synthesized with zinc nitrate (ZnO$_A$), then ZnO$_N$-MN is found, the treatments obtained with the acetate salt showed less damage to red cells, however, although the concentrations used do not exhibit hemolysis percentages greater than 3%, if they affect the morphology of the cell from 25 µg/mL, elongated oval shapes can be observed and at 100 µg/mL powder saturation can be observed at 40x and different morphologies known as echinocytes. Particularly for biomaterials, up to 5% of hemolysis is considered as non-hemolytic [49, 50], the above-mentioned results do not show such an effect without the embryo, the presence of an abnormality in erythrocyte morphologies is not adequate since the echinocyte form shows the development of acute hemolysis and this being associated in non-immune *hemolytic* anemias [51]. However, there are studies with ZnO synthesized by different methods that do not promote the breakdown of red blood cells at concentrations less than 100 µg/mL [52], could confirming that both the process and the resulting products in sol–gel under the conditions studied are toxic (Fig. 5).

## Conclusion

1. Morphological differences were found according to the ZnO precursor used, as well as the incorporation of MG allows to reduce the aging of the gel and with it the reduction of the particle size.

2. No treatment showed a significant difference ($p < 0.05$) in the antitopoisomerase activity test but, this type of nanoparticles has antimicrobial activity in other studies.
3. The treatments synthesized with zinc acetate showed greater affinity for COX-II than for COX-II, being the one loaded with mangiferin the one that showed the best result, on the other hand, those obtained with zinc nitrate did not show favorable results associated with a selective anti-inflammatory effect of COX.-II.
4. $ZnO_A$-MG also showed less damage in HEPG2 and BEAS-2B, the most toxic were the treatments synthesized with zinc nitrate showing discrepancies between the loaded and unloaded.
5. All treatments generate morphological changes of erythrocytes but $ZnO_N$ showed a higher percentage of hemolysis compared to the rest.

In general, these results show that ZnO with both precursors generates cyto and hepatoxicity in addition to promoting anemic difficulties, therefore, treatment concentrations should be considered considering biological activity and cytotoxic effect before considering an application as a nutraceutical however, their antibacterial activity can be a good option in other studies. Moreover, mangiferin significantly reduces ($p < 0.05$) the toxic effects of NP's, which confirms its presence in the nanoparticle.

**Acknowledgements** The FFR-C student thanks the National Council of Science and Technology of Mexico (CONACYT) for the grant number 787023 awarded for the development of postgraduate studies

## Compliance with Ethical Standards

**Conflicts of interest** The authors declare no conflict of interest.

## References

1. Q. Yuan, S. Hein, and R. D. K. Misra (2010). *Acta Biomater.* **6**, (7), 2732–2739.
2. J. Wright and N. Sommerdijk *Sol-Gel Materials Chemistry and Applications* (Gordon & Breach Science, London, 2010).
3. G. Rodríguez-Gattorno, P. Santiago-Jacinto, L. Rendon-Vázquez, J. Németh, I. Dékány, and D. Díaz (2003). *J. Phys. Chem. B* **107**, (46), 12597–12604.
4. Y. S. Fu, et al. (2007). *J. Am. Chem. Soc.* **129**, (51), 16029–16033.
5. Z. R. Khan, M. S. Khan, M. Zulfequar, and M. Shahid Khan (2011). *Mater. Sci. Appl.* **2**, (5), 340–345.
6. C. B. Ong, L. Y. Ng, and A. W. Mohammad (2018). *Renew. Sustain. Energy Rev.* **81**, (1), 536–551.
7. M. F. Khan, et al. (2016). *Sci. Rep.* **6**, (March), 1–12.
8. A. Sirelkhatim, et al. (2015). *Nano-Micro Lett.* **7**, (3), 219–242.
9. A. C. Anselmo and S. Mitragotri (2016). *Bioeng. Transl. Med.* **1**, (1), 10–29.
10. F. H. Chalé, D. B. Ancona, and M. R. S. Campos (2014). *Nutr. Hospital.* **29**, (1), 10–20.
11. N. Saha and S. D. Gupta (2016). *J. Clust. Sci.* **27**, (4), 1419–1437.
12. J. M. Carbonell-Capella, M. Buniowska, F. J. Barba, M. J. Esteve, and A. Frígola (2014). *Comprehens. Rev. Food Sci. Food Saf.* **13**, (2), 155–171.
13. A. Vyas, K. Syeda, A. Ahmad, S. Padhye, and F. H. Sarkar (2012). *Mini-Rev. Med. Chem.* **12**, (5), 412–425.
14. A. J. Núñez Sellés, et al. (2002). *J. Agric. Food Chem.* **50**, (4), 762–766.
15. H. Liu, et al. (2011). *J. Pharm. Biomed. Anal.* **55**, (5), 1075–1082.
16. F. Gold-Smith, A. Fernandez, and K. Bishop (2016). *Nutrients* **8**, (7), 16–20.
17. P. Uikey and K. Vishwakarma (2016). *Int. J. Emerging Technol. Comput. Sci. Electron. (IJETCSE)* **21**, (2), 976–1353.
18. A. Khansari, M. Enhessari, and M. Salavati-Niasari (2013). *J. Clust. Sci.* **24**, (1), 289–297.
19. R. Kumar, A. Umar, G. Kumar, and H. S. Nalwa (2017). *Ceram. Int.* **43**, (5), 3940–3961.
20. J. Nitiss and J. C. Wang (1988). *Proc. Nat. Acad. Sci.* **85**, (20), 7501–7505.
21. J. L. Nitiss and K. C. Nitiss (2003). *DNA Topoisome. Protoc.* **95**, (1), 315–328.
22. N. Chatterjee, et al. (2014). *J. Toxicol. Environ. Health Part A* **77**, (11), 1399–1408.
23. N. Chatterjee, J. S. Yang, K. Park, S. M. Oh, J. Park, and J. Choi (2015). *Environ. Health Toxicol.* **30**, e2015007.
24. A. Pérez-Larios, R. Lopez, A. Hernández-Gordillo, F. Tzompantzi, R. Gómez, and L. M. Torres-Guerra (2012). *Fuel* **100**, 139–143.
25. K. Hatanaka, et al. (1999). *Life Sci.* **65**, (13), 161–166.
26. Y. Harada, et al. (1996). *Prostaglandins* **51**, (1), 19–33.
27. F. F. Razura-Carmona, et al. (2019). *Cancers* **11**, (1965), 1–17.
28. M. B. Hansen, S. E. Nielsen, and K. Berg (1989). *J. Immunol. Methods* **119**, (2), 203–210.
29. J. Javidi, A. Haeri, F. H. Shirazi, F. Kobarfard, and S. Dadashzadeh (2017). *J. Clust. Sci.* **28**, (1), 165–178.
30. Z. Yufei, G. Zhiyou, G. Xiaoqi, C. Dongxing, D. Yunxiao, and Z. Hongtao (2010). *J. Semicond.* **31**, (8), 1–6.
31. S. H. Jung, et al. (2008). *Cryst Growth Design* **8**, (1), 265–269.
32. Y. R. Corrales-Ureña, et al. (2017). *Perspect. Invest.* **7**, (1), 8–16.
33. S. Rajeshkumar, S. V. Kumar, A. Ramaiah, H. Agarwal, T. Lakshmi, and S. M. Roopan (2018). *Enzyme Microb. Technol* **117**, 91–95.
34. M. Pudukudy and Z. Yaakob (2015). *J. Clust. Sci.* **26**, (4), 1187–1201.
35. A. Pona, A. Cline, S. S. Kolli, S. L. Taylor, and S. R. Feldman (2019). *Dermatol. Therapy* **32**, (2), 1–21.
36. Y. Zu, et al. (2011). *Int. J. Mol. Sci.* **12**, (7), 4237–4249.
37. C. Sheng, Z. Miao, and W. Zhang (2016). *Stud. Nat. Product. Chem.* **47**, (2), 1–28.
38. A. M. Youssef, A. M. El-Nahrawy, and A. B. Abou-Hammad (2017). *Int. J. Biol. Macromol.* **97**, 561–567.
39. A. Nejabatdoust, A. Salehzadeh, H. Zamani, and Z. Moradi-Shoeili (2019). *J. Clust. Sci.* **30**, (2), 329–336.
40. Y. Gao, et al. (2019). *J. Clust. Sci.* **30**, (4), 937–946.
41. M. G. Moro, et al. (2019). *Braz. Dental J.* **30**, (2), 133–138.
42. T. SivaKumar, A. ShobhaRani, K. Sujatha, B. Purushotham, and P. Neeraja (2017). *Asian J. Pharm. Clin. Res.* **10**, (1), 313–316.
43. M. Sumalatha, et al. (2015). *Nat Product Commun.* **10**, (10), 1703–1704.
44. Y. Zhou, et al. (2017). *Nanomaterials* **7**, (4), 1–15.
45. U. Kadiyala, E. S. Turali-Emre, J. H. Bahng, N. A. Kotov, and J. ScottVanepps (2018). *Nanoscale* **10**, (10), 4927–4939.
46. R. Sivaraj, P. K. S. M. Rahman, P. Rajiv, S. Narendhran, and R. Venckatesh (2014). *Spectrochim. Acta-Part A* **129**, 255–258.

47. B. C. Heng, X. Zhao, S. Xiong, K. W. Ng, F. Y. Boey, and J. S. Loo (2010). *Food Chem. Toxicol.* **48**, (6), 1762–1766.
48. L. Künzi, et al. (2015). *Sci. Rep.* **5**, 1–10.
49. L. H. Zhao, R. Zhang, J. Zhang, and S. Q. Sun (2012). *CrystEngComm* **14**, (3), 945–950.
50. J. P. Singhal and A. R. Ray (2002). *Biomaterials* **23**, (4), 1139–1145.
51. J. Gay, L. Garçon, and P. Coppo (2016). *EMC-Tratado de Medicina* **20**, (4), 1–7.
52. M. Rajapriya, et al. (2019). *J. Clust. Sci.* **6**, 791–801.